END

FILMED

DTIC

MICROCOPY RESOLUTION TEST CHART

NATIONAL BUREAU OF STANDARDS-1963-A

Crystallization Behavior of

Poly[3,3-bis(ethoxymethyl) oxetane]

and Poly[3,3-bis(azidomethyl) oxetane]

K. E. Hardenstine[+], G. V. Henderson, Jr., L. H. Sperling[+]
and C. J. Murphy[*]

Polymer Science and Engineering Program
Lehigh University
Materials Research Center
Bethlehem, PA 18015

[+]Department of Chemical Engineering
[*]Permanent Address: East Stroudsburg University
East Stroudsburg, PA 18301

and

G. E. Manser
Thiokol Wasatch Division
Brigham City, Utah 84302

NOV 2 8 1984

A

Acknowledgement

Abstract

Two crystal modifications have been found for poly [3,3-bis(ethoxymethyl) oxetane], poly(BEMO), by wide-angle x-ray powder diffraction and differential scanning calorimetry while only one modification has been found for poly[3,3-bis(azido methyl) oxetane], poly(BAMO). Melting temperatures for the two polymers were nearly the same, varying from about 70°C to about 90°C depending on the thermal treatment; higher crystallization temperatures resulted in higher melting temperatures. The equilibrium melting temperature, T_m^*, was found to be 125°C and 128°C for poly(BEMO) and poly(BAMO), respectively, using the Hoffman-Weeks extrapolation procedure. Measurement of the melting point depression of poly(BEMO) and poly(BAMO) in di-butyl phthalate yielded enthalpy of fusion values of 2.25 kcal/mole and 12.8 kcal/mole, respectively. The percent crystallinity for poly(BEMO) and poly(BAMO), respectively was calculated to be 55-60% and 13-30% based on DSC and x-ray analysis.

Introduction

This paper is the third in a series regarding the studies of homopolymers and block copolymers based on poly[3,3-bis(ethoxymethyl) oxetane], poly(BEMO), poly [3,3-bis(azidomethyl)oxetane], poly(BAMO), and other novel polyethers (1,2). In the present work, the melting behavior of poly(BEMO) and poly(BAMO) homopolymers as prototype crystalline hard blocks was studied under various crystallization conditions.

While the crystalline structures of poly(BEMO) and poly(BAMO) have not been reported, numerous studies have been done on other polyoxetanes. Tadokoro et al. (3-7) published a series of papers on the structures of polyethers, finding three crystal modifications for polyoxetane. The first modification was essentially planar zigzag all trans TTTT and stable only in the presence of water. Modification II was stable only as oriented samples as a combination of trans and gauche, T_3GT_3G. The third modification was the most stable form, $(T_2G_2)_2$, consistent with the antiparallel arrangement of the strong dipole-moments of the COC groups.

Pérez et al. (8) studied the influence of the crystallization temperature on the melting behavior and crystalline structure of several polyoxetanes.

1.

Poly[3,3-(dimethyl)oxetane], PDMO, and poly[3,3-(diethyl)oxetane], PDEO, were isothermally crystallized at various temperatures and analyzed by differential scanning calorimetry (DSC) and x-ray analysis. When PDMO was isothermally crystallized below 0°C only one DSC peak was present, but when the crystallization temperatures were in the range of 0°C to 16°C two DSC peaks were discerned. At crystallization temperatures higher than 16°C, only one peak was again observed. Similar behavior was seen for PDEO.

In work related to the present study, Nakagawa and Ishida (9) used various crystallization and heat treatments to study the melting behavior and crystalline structure of poly(vinylidene fluoride). They found that the melting behavior depended strongly on the annealing conditions.

Crystalline Block Copolymers

Morton, et al. (10,11) pointed out block copolymers of the ABA or {AB}$_n$ types need not have glassy hard blocks for good properties, and that crystalline hard blocks offered special advantages. These include the possibility of having the A and B blocks being mutually miscible in the melt, with the A blocks capable of crystallizing on cooling. Thus, lower melt viscosities are achieved while maintaining the thermoplastic elastomer characteristics at room temperature.

Recently, Goodman and Vachon (12,13) studied the crystalline character and mechanical properties of anionic block copolymers of ε-caprolactam with ε-caprolactone. Perego et al. (14-16) have carried out an extensive investigation of the structural and morphological features of poly(ester esteramide)s based on poly(ester amide) "hard" segments and poly(tetramethylene oxide) "soft" segments. They also studied poly(ether ester)s based on poly(tetramethylene terephthalate) "hard" segments and poly(tetramethylene oxide). As the softening or melting behavior of these block copolymers is governed by the "hard" segment, the crystalline structure and thermodynamic properties of the "hard" segments demand special attention.

3.

Of course, the above only touches on the extensive literature of crystalline polymers. Tadokora recently reviewed the subject in some detail (6).

4.

Experimental

Materials

Burdick and Jackson UV grade THF and methylene chloride were dried and stored over molecular sieves. Commercial grade boron trifluoride etherate was freshly distilled in vacuo before use. 1,4-Butanediol was distilled from calcium hydride and stored over molecular sieves.

3,3,-bis(ethoxymethyl) oxetane, BEMO, monomer was prepared by the reaction of sodium ethoxide with 3,3-bis(chloromethyl) oxetane (17) in refluxing methanol. 3,3-bis(azidomethyl) oxetane, BAMO, monomer was likewise prepared by the reaction of sodium azide with 3,3-bis(chloromethyl) oxetane in refluxing methanol. Both monomers were freshly distilled from calcium hydride before use. All glassware was flame dried and swept with nitrogen immediately preceeding the introduction of reactants. During polymerization the reactants were maintained under a dry nitrogen atmosphere.

The solution polymerization of poly(BEMO) or poly(BAMO) proceeds as follows (18). 100 grams of calcium hydride dried methylene chloride is charged into a flame dried 500 cm^3 resin flask which is maintained under a nitrogen atmosphere. To this flask, the

5.

calculated amount of freshly distilled 1,4-butanediol is then added, followed by the calculated amount of boron trifluoride etherate in the mole ratio of 1:2. This solution is allowed to react for 1 hour at room temperature. The reactor is then cooled to $-10^{\circ}C$ and after 30 minutes a solution of monomer is added dropwise in methylene chloride (25% w/w concentration). The time of addition usually ranges from 20 minutes to 2 hours. After a conversion of 90% is reached, the contents of the flask are quenched with 50cc of saturated brine solution. The organic phase is separated off, washed with 10% sodium bicarbonate solution, dried over magnesium sulfate and evaporated to dryness at room temperature. The resultant polymer is purified by precipitation from cold methanol. The homopolymers used in this study, their structures and abbreviations are shown in Table I. The structures of both homopolymers were confirmed by elemental analysis, Table II.

Instrumental

The molecular weights of the homopolymers were estimated by intrinsic viscosity using an Ubbelhode viscometer with methylene chloride as solvent at $25^{\circ}C$. The molecular weights were also estimated by gel permeation chromatography (GPC) using a Waters GPC calibrated with poly(tetrahydrofuran) standards.

6.

All DSC measurements were made on a Perkin-Elmer DSC 1-B. Calibration was made using indium ($T_m = 429^\circ K$) and tin ($T_m = 505^\circ K$) standards obtained from Perkin-Elmer. In all cases sample sizes were 5-10 mg. The samples were all placed in aluminum pans, weighed, and crimped. The sample pan was then placed in one sample holder while a Perkin-Elmer reference pan was placed in the other.

X-ray powder diffraction studies employed a Phillips APD 3600 automated x-ray powder diffractometer with a copper target and a Phillips XRG x-ray generating unit. A nickel filter was used to isolate the CuKα line, $\lambda = 1.542 \overset{\circ}{A}$. The scan rate was 1.0°/min by increments of 0.02°.

Density measurements were obtained by volume displacement at room temperature in a pycnometer.

Polymer - diluent mixtures were prepared for measurement of the melting point depression. A 0.1 g portion of polymer, accurately weighed, and the desired amount of diluent, di-n-butyl phthalate (DBP) were heated to 100° C overnight to ensure complete mixing between polymer and diluent. The samples were cooled slowly from the melt. Melting temperatures were measured by DSC at a heating rate of 10° C/min.

7.

Theory

As pointed out some years ago by Flory (19), the melting point depression of a semicrystalline polymer due to the presence of a low molecular weight diluent of volume fraction v_1 may be written as:

$$(1/T_m) - (1/T_m°) = (R/\Delta H_f)(V_u/V_1)[v_1 - (BV_1/RT_m)v_1^2] \qquad (1)$$

Here T_m and $T_m°$ are the melting points in the presence and absence of the diluent, respectively, ΔH_f and V_u are the heat of fusion and volume per mole of repeating unit, V_1 is the molar volume of the diluent, R is the gas constant, and B is the polymer solvent interaction parameter. This relation permits the heat of fusion to be evaluated from melting point depression data. The measurements are customarily performed on samples which have been slowly cooled from the melt. It was confirmed that this procedure does not lead to large errors in calculations of ΔH_f (20).

Part I - Characterization

The intrinsic viscosity of poly (BEMO) at 25° C was found to be 26.2 ml/gram and 15.7 ml/gram for poly (BAMO). The molecular weight distribution data determined by GPC using poly (tetrahydrofuran) as the calibration standard are listed in Table III. The density of poly (BEMO) at 25° C was found to be 0.85 gm/cm^3 0.92 gm/cm^3 for poly (BAMO).

Part II - Melting Behavior

As - Received

Figures 1 and 2 show the DSC thermograms for as-received poly (BEMO) and poly (BAMO) at 10° C/min respectively. Poly (BEMO) has three peaks at 63° C, 75° C, and 77° C and a melting temperature of 80° C where the last trace of crystallinity disappears and there is a return to the baseline. Poly (BAMO) has two peaks at 78° C and 82.5° C and a melting temperature of 87.5° C.

Both the as-received poly (BEMO) and poly (BAMO) were heated to 100° C and allowed to cool slowly to room temperature. Both samples showed a single melting peak upon reheating. Poly (BEMO) then melted in the range of 78-80° C and poly (BAMO) in the range of 87-90° C.

9.

Quench Crystallized

When the samples of poly (BEMO) and poly (BAMO), are quickly quenched in liquid nitrogen from the melt state, the DSC curves at a heating rate of 10° C/min. show two thermal transitions: an exothermic peak near 5° C corresponding to cold crystallization and an endothermic peak with T_m at 75° C (Poly BEMO) and 85° C (Poly BAMO), see Figure 3.

Isothermally Crystallized Specimens

Poly (BEMO) and poly (BAMO) samples were heated above their melting temperatures and allowed to crystall-ize isothermally at various temperatures. The effect of crystallization temperature on the remelting temperature was then determined. When poly (BEMO) is undercooled from the melt to different crystallization temperatures, the DSC curves show that the melting temperature decreases as the crystallization tempera-ture decreases (Figure 4). The poly (BEMO) polymer shows only a single melting endotherm, independent of the crystallization conditions. T_m varies between 82° C and 76° C as the crystallization temperature was lowered from 50°C to -6°C.

Similar results were obtained for poly (BAMO). The melting temperature decreased with a decrease in

10.

the crystallization temperature. A single melting
endotherm was seen for each crystallization temperature.
The melting temperature varied between 90° C and 87° C
as the crystallization temperature was reduced from
50° C to -6° C.

Solution Crystallized Specimens

In an attempt to recover the multiple melting
peak conditions, samples of poly (BEMO) and poly (BAMO)
were dissolved in methylene chloride. These solutions
were slowly dripped into methanol held at various
temperatures. (This experiment simulated initial
crystallization during synthesis). The polymers were
allowed to crystallize in solution for approximately
one day. The samples were dried in a vacuum oven at
room temperature until constant weight.

Figure 5 displays the (DSC, 10° C/min) thermograms
for poly (BEMO) crystallized as above at -25° C, 0° C
and 25° C. All of the samples have a melting tempera-
ture of 78° C. Samples of poly (BAMO) were crystallized
at 0° C and 25° C. The thermograms for poly (BAMO) (not
shown) are similar to that of poly (BEMO) with a single
melting peak and melting temperatures of 87.5° C.

11.

Part III - Thermodynamics of Crystallization

Equilibrium Melting Point

Figure 6 shows the effect of crystallization temperature, T_c, on the observed melting temperature, T_m, for poly (BEMO). In this study, the samples were maintained above their melting points for at least 30 minutes to ensure complete melting of the crystals before being cooled at 10° C/minute to the crystallization temperature (21). Following the crystallization treatment at T_c, the samples were cooled to room temperature at 10° C/minute. In the last cooling run, thermograms of the samples failed to reveal any evidence of secondary crystallization. In the final part of the program, the melting temperatures of the isothermally crystallized samples were measured at 10° C/minute.

By using the Hoffman-Weeks extrapolation procedure (22,23), T_m^* (the equilibrium melting temperature) can be determined from the intersection of the experimental plot of T_m versus T_c with the line representing $T_m = T_c$. The equilibrium melting temeprature for poly(BEMO) is 125°C and 128°C for poly(BAMO).

12.

If it is assumed that the crystals are perfect
and of finite size and that no recrystallization takes
place during the melting run, the experimental data in
Figure 6 can be described by an equation for isothermal
crystallization (22,24)

$$T_m^* - T_m = \emptyset \ (T_m^* - T_c) \qquad (2)$$

where $\emptyset$ is the stability parameter which depends on
the crystal thickness. In equation (2), where $\emptyset$
assumes all values between 0 and 1, $\emptyset = 0$ implies
$T_m = T_m^*$ for T_c whereas $\emptyset = 1$ implies $T_m = T_c$.
Therefore, the crystals are most stable at $\emptyset = 0$ and
inherently unstable at $\emptyset = 1$. For poly BEMO, $\emptyset = 0.55$
and $\emptyset = 0.39$ for poly(BAMO), suggesting that the crystals
are stable to a normal degree.

Enthalpy of Fusion

According to equation (1), $[(1/T_m)-(1/T_m^\circ)]/v_1$
is plotted as a function of v_1/T_m for poly(BEMO),
see Figure 7. The values of 2.25 kcal/mole of repeat
units and 1.45 cal/cm^3 for ΔH_f and B for poly (BEMO)
were calculated from the intercept and slope of the line,
respectively. The values of 12.8 kcal/mole for ΔH_f
and 6.32 cal/cm^3 for B were similarly calculated for poly
(BAMO). Since the equilibrium melting temperature T_m^*
for poly (BEMO) is 125° C, the equilibrium entropy of
fusion, ΔS, can be calculated from $\Delta S = \Delta H_f/T_m^*$,

13.

and is found to be 5.6 eu/mole of repeat units. The equilibrium entropy of fusion for poly (BAMO) is 32.0 eu/mole of repeat units.

The percent crystallinity can be calculated from

$$X_{cr} = \frac{\Delta H_f}{\overline{\Delta H_f}} \tag{3}$$

where ΔH_f is the observed specific enthalpy of fusion determined from the area under the DSC thermogram. The quantity $\overline{\Delta H_f}$ is the specific enthalpy of fusion of the crystalline phase as it exists in the polymer and is determined by melting point depression data. (23). The observed specific enthalpy by DSC of poly (BEMO) and poly (BAMO) were found to be 1.24 kcal/mole and 1.66 kcal/mole respectively. Therefore the percent crystallinity as determined by equation (3) for poly (BEMO) is 55% and 13% for poly (BAMO).

Part IV - X-Ray Results

Apparent Degree of Crystallinity

Figures 8 and 9 are x-ray diffractograms of poly (BEMO) and poly (BAMO), respectively. Figure 8b shows a wide-angle x-ray powder diffractometer scan of as-received poly (BEMO). The apparent degree of crystallinity is defined as

$$X_{cr}' = 1_c/(I_c + I_a) \tag{4}$$

where I_c and I_a are the areas under crystalline peaks

14.

and amorphous peaks, respectively, after correcting the intensity for incoherent scattering (25). The apparent degree of crystallinity was found to be 60% for poly (BEMO) and 30% for poly (BAMO). These values are in fairly good agreement with the calorimetric estimates of crystallinity, see previous section.

As Received vs. Melt Crystallized Samples

The as-received poly (BEMO) sample, Figure 8b has been designated Modification II and the sample crystallized from the melt, Figure 8a, Modification I. There are major differences between these x-ray diffractograms. Both samples have major peaks at approximately 2θ = 8.6, 16.0, 19.1 and 22.3, yet the sample crystallized from the melt has lost the peaks at 2θ = 11.9, 12.5 and 21.1. These differences are delineated in Table IV.

The as-received poly (BAMO) and the melt-crystallized sample have nearly identical x-ray scans as shown in Figure 9 and 11 in Table IV. It must be emphasized that there were no peaks lost on recrystallizing poly BAMO.

Samples of poly (BEMO) crystallized in solution at various temperatures (Figure 5) were also examined by x-ray methods. The scans of the samples crystallized

15.

at -25° C, 0° C and 25° C were found to be Modification I.
The samples crystallized from the melt isothermally at
various temperatures (Figure 4) were also found to exist
as Modification I.

Discussion

Multiple endotherms are frequently found on DSC scans in the melting region of semicrystalline polymers. This behavior is shown in Figures 1 and 2 for as-received poly (BEMO) and poly (BAMO), respectively. Several interpretations have been presented for this phenomenon (26 - 28), depending on the results of supporting experiments. Some of these include that the lower-temperature endotherm does not correspond to the melting of a crystalline phase, but rather to a solid-solid phase transition, or partial melting, and that the higher temperature endotherm indicates melting of the crystalline phase formed by such transitions as orientation changes of crystals, phase transition be-tween crystalline modificiations or recrystallization (29). Multiple peaks have also been ascribed to hetero-geneity of molecular weight, heterogeneity in crystall-ite size or to the formation of two coexisting crys-talline forms.

Figure 3 displays recrystallized poly (BEMO) and poly (BAMO) at high undercoolings with a single melting peak. Therefore, it might be deduced that the multiple fusion peaks of Figures 1 and 2 typify imposed crystallization conditions, and are the result of a

17.

distribution of crystallite sizes due to restricted crystallization caused by the heterogeneities.

The poly (BAMO) samples had identical x-ray diffraction scans (Figure 9) suggesting that the multiple fusion peaks in Figure 2 are the result of heterogeneities in crystallite sizes and that a single crystalline modification exists. However, x-ray analysis on as-received vs. melt-crystallized samples of poly(BEMO) indicated the presence of two crystalline structures (Figure 8).

Two types of experiments were carried out in an attempt to separate the two different crystalline modifications of poly (BEMO). Isothermal crystallization was successful for Pérez et al. (8) on similar polyoxetanes. When similar isothermal crystallization experiments were performed on poly (BEMO), single melting endotherms with about the same T_m were found for all crystallization temperatures (Figure 4). These results suggest that a single crystalline modification exists when the polymer is isothermally crystallized from the melt. This was confirmed by x-ray analysis and found to be Modification I.

Considering that the as-received poly (BEMO) had multiple peaks when crystallized from solution, the second experiment was to recrystallize the poly (BEMO)

18.

in methanol at various temperatures. Again, a single melting endotherm for all crystallization temperatures was present with identical T_m's indicating only one crystalline modification. This was also confirmed by x-ray analysis.

The crystal structures of poly (BEMO) and poly (BAMO) have not been described to date. As seen in Table I, the backbone structures of poly (BEMO) and poly (BAMO) are identical to the skeletal bonds of poly (oxetane). According to Tadokoro, et. al. (4), the backbone structure of poly (oxetane) may assume three possible conformations. Of the three models, one TTTT is all planar zigzag.

$$- CH_2 \{ 0 - CH_2 - CH_2 - CH_2 \}_n -$$

$$\begin{array}{cccc} T & T & G & G \\ T & T & T & G \\ T & T & T & T \end{array}$$

(5)
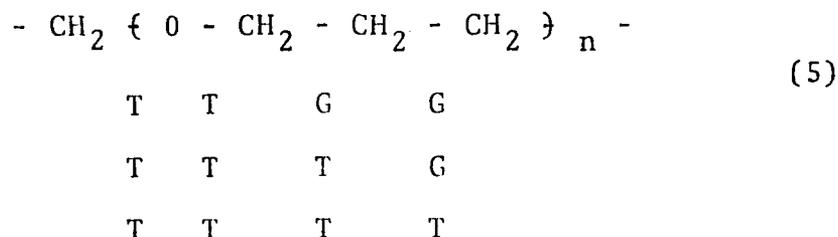
The second model is the TTTG type, in which two C-O bonds and one C-C bond are trans and the other C-C bond is gauche. The third model is the TTGG. Two C-O bonds are trans and two C-C bonds are gauche. The following arguments have been taken into account here: (1) the C-O bond in these polymers cannot take the gauche form,

19.

because of the short distance between the attached two CH_2 groups. (2) The C-C bond can take either of the two forms, trans or gauche. All these molecular conformations have been found for poly (oxetane). These three molecular conformations may also be considered as the backbone structure of poly (BEMO) and poly (BAMO). Tadokoro et al. calculated the fiber axis length to be 4.80 Å for the planar zigzag TTTT model. Since both the poly (BEMO) and poly (BAMO) x-ray diffractograms showed a large peak at about $2\theta = 19^O$ (d = 4.75 Å) the planar zigzag model may tentatively be considered as the structure of the backbone of these polymers (30).

Conclusions

Two crystalline modifications have been found for poly (BEMO). When the poly (BEMO) samples are crystallized from the melt or solution at various temperatures, modification I exists. Modification II has been found in the as-received samples but has not been reproduced from the original sample at this time. Poly (BAMO) samples underwent similar experiments as the poly (BEMO) samples and a single crystalline form was found to exist.

The enthalpy of fusion was calculated for poly (BEMO) and poly (BAMO) and found to be 2.25 kcal/mole and 12.8 kcal/mole, respectively. The increase in the enthalpy of poly (BAMO) is most likely due to the greater polarity of the azido side groups. While the melting temperatures of the two polymers varied from about 70°C to about 90°C depending on crystallization conditions, the equilibrium melting temperatures were found to be 125°C and 128°C for poly(BEMO) and poly(BAMO), respectively.

The results of this work provide important engineering data for the development of thermoplastic elastomer block copolymers based on crystallizable polyethers. Melting temperatures in the range of 70-100 °C, followed by low melt viscosities are important for many adhesive and binder applications, for example.

21.

References

1. R. B. Jones, C. J. Murphy, L. H. Sperling, M. Farber, S. P. Harris and G. E. Manser, J. Applied Polym. Sci. accepted (1984).

2. K. E. Hardenstine, C. J. Murphy, R. B. Jones, L. H. Sperling, and G. E. Manser, J. Applied Polym. Sci., accepted (1984).

3. H. Kakida, D. Makino, Y. Chatini, M. Kobayashi and H. Tadokoro, Macromolecules, 3, 569 (1970).

4. H. Tadokoro, Y. Takahashi, Y. Chatani, and H. Kakida, Makromol. Chem. 109, 96 (1967).

5. Y. Takahashi, Y. Osaki, H. Tadokoro, J. Polym. Sci. Polym. Phys. Ed. 18, 1863 (1980).

6. H. Tadokoro, "Structure of Crystalline Polymers", Wiley Interscience, New York (1979).

7. H. Tadokoro, Polymer, 25 (2), 147 (1984).

8. E. Pérez, M. A. Gómez, A. Bello, and J. G. Fatou, Colloid and Polymer Sci., 261, 571 (1983).

9. K. Nakagawa and Y. Ishida, J. Polym. Sci. Polym. Phys. Ed. 11, 2153 (1973).

10. M. Morton, Rubber Chem. Tech., 56, 1096 (1983).

11. M. Morton, N. C. Lee, and E. R. Terrill, Ch. 5 in "Elastomers and Rubber Elasticity", J. E. Mark and J. Lal, Eds., American Chemical Society, Washington, D. C., 1982.

22.

12. I. Goodman and R. N. Vachon, Eur. Polym. J.,
    20, 539 (1984).

13. I. Goodman and R. N. Vachon, Eur. Polym. J., 20,
    529 (1984).

14. E. Sorta and G. della Fortuna, Polymer 21,
    728 (1980).

15. G. Perego, M. Cesari, and G. della Fortuna, J.
    Appl. Polym. Sci., 29, 1141 (1984).

16. G. Perego, M. Cesari, and R. Vitali, J. Appl.
    Polym. Sci., 29, 1157 (1984).

17. W. Carpenter, U.S. Patent 3,183,609 (1984).

18. G. E. Manser, (Thiokol) U.S. Patent 4,393,199
    (1983).

19. P. J. Flory, J. Chem. Phys. 17, 223 (1949).

20. W. R. Krigbaum and I. Uematsu, J. Polym. Sci. A,
    3, 767 (1965).

21. T. Nishi and T. T. Wang, Macromolecules, 8, 909
    (1975).

22. J. D. Hoffman and J. J. Weeks, J. Res. Natl. Bur.
    Stand. 66A, 13 (1962).

23. L. Mandelkern, J. Polym. Sci., 47, 494 (1960).

24 L. Mandelkern, "Crystallization of Polymers",
    McGraw-Hill, New York, NY (1964).

25. S. Kavesh and J. M. Schultz, Polym. Eng. and Sci.,
     $\underline{9}$, 452 (1969).

26. M. Jaffe and B. Wunderlich, Kolloid Z.Z. Polym.,
     $\underline{216\text{-}217}$, 203 (1967).

27. J. P. Bell, P. E. Slade and J. H. Dumbleton, J.
     Polym. Sci. $\underline{A\text{-}2}$, $\underline{6}$, 1773 (1968).

28. J. P. Bell, J. H. Dumbleton, J. Polym. Sci. $\underline{A\text{-}2}$,
     $\underline{7}$, 1033 (1969).

29. S. F. Bermudez and J. G. Fatou, European Polymer
     Journal, $\underline{8}$, 575 (1972).

30. L. V. Azaroff and M. J. Buerger, "The Powder
     Method in X-ray Crystallography", McGraw-Hill,
     NY (1958).

24.

Table Captions

Table I.   Polyether Structures.

Table II.   Elemental Analysis Results.

Table III.   Molecular Weight Distribution Data for Poly(BEMO) and Poly(BAMO) samples[a].

Table IV.   Values of 2θ for Various Poly(BEMO) and Poly(BAMO) Samples.

25.

Figure Captions

Figure 1. DSC thermogram of as-received poly(BEMO).

Figure 2. DSC thermogram of as-received poly(BAMO).

Figure 3. DSC thermograms of poly(BEMO) and poly(BAMO)
           quenched in liquid nitrogen.

Figure 4. Dependence of melting temperature on iso-
           thermal crystallization temperature for
           poly(BEMO).

Figure 5. DSC thermograms of poly(BEMO) crystallized
           in solution at various temperatures.

Figure 6. Equilibrium melting point determination by
           a plot of T_m vs. T_c for poly(BEMO).

Figure 7. Enthalpy of fusion determination by diluents
           for mixtures of poly(BEMO) and dibutyl
           phthalate (DBP).

Figure 8. Modification I and II of poly(BEMO) as seen
           by wide-angle powder diffraction. Units of
           intensity are arbitrary.

Figure 9. Wide-angle X-ray powder diffraction scan of
           poly(BAMO). Units of intensity are arbitrary.

26.

Table I. Polyether Structures.

Name	Abbreviation	Structure
poly[3,3-bis(ethoxymethyl)oxetane]	poly(BEMO)	$\{O-CH_2-\underset{\underset{CH_2-O-CH_2-CH_3}{\mid}}{\overset{\overset{CH_2-O-CH_2-CH_3}{\mid}}{C}}-CH_2\}_m$
poly[3,3-bis(azidomethyl)oxetane]	poly(BAMO)	$\{O-CH_2-\underset{\underset{CH_2N_3}{\mid}}{\overset{\overset{CH_2N_3}{\mid}}{C}}-CH_2\}_m$

Table II. Elemental Analysis Results.

	Poly(BEMO)		Poly(BAMO)	
	Experimental	Theoretical	Experimental	Theoretical
%C[a,b]	61.55	62.07	36.10	35.71
%H	10.48	10.34	4.75	4.76
%O	27.97	27.59	9.50	9.53
%N	-----	-----	49.60	50.00

a) All percentages are on a weight basis.

b) Analyses performed by: G.I. Robertson
Microanalytical Lab
73 West End Ave.
Florham Park, NY 07932

28.

Table III. Molecular Weight Distribution Data for

Poly(BEMO) and Poly(BAMO) Samples[a].

	$\overline{M}_n$	$\overline{M}_w$	$\overline{M}_w/\overline{M}_n$	$[\eta]\ \frac{cm^3}{gm}$
Poly(BEMO)	22,600	73,500	3.25	26.2
Poly(BAMO)	25,000	50,800	2.03	15.7

[a]$\overline{M}_n$, $\overline{M}_w$ represent number and weight average molecular weights calculated from gel permeation chromatography calibrated with poly(tetrahydrofuran) standards.

29.

Table IV. Values of 2θ for Various Poly(BEMO) and Poly(BAMO) Samples.

Poly(BEMO)		Poly(BAMO)	
2θ(As-Received)	2θ(Melt Crystallized)	2θ(As-Received)	2θ(Melt Crystallized)
8.57	8.64	11.69	11.86
9.52	9.57	15.31	15.56
11.90	-----	16.41	16.63
12.53	-----	19.26	19.55
15.95	15.90	23.68	23.80
17.26	17.18	26.79	27.10
19.09	19.02	28.27	28.51
20.14	20.10	31.02	31.29
21.13	-----	33.32	33.60
22.27	22.24	39.75	39.24
23.97	23.24	43.32	43.17
72.50	72.30	72.65	72.54

30.

DSC of As-Received Poly[BEMO]
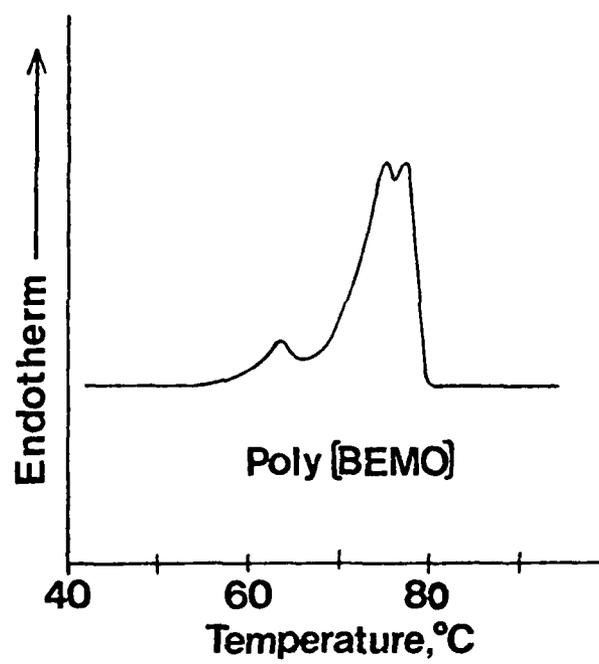
FIGURE 1

DSC of As-Received Poly[BAMO]

FIGURE 2

DSC of Quenched Polyethers
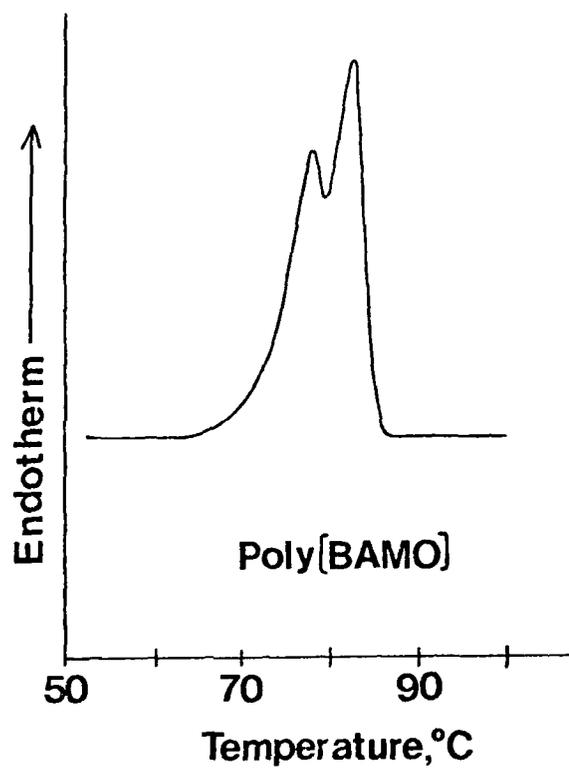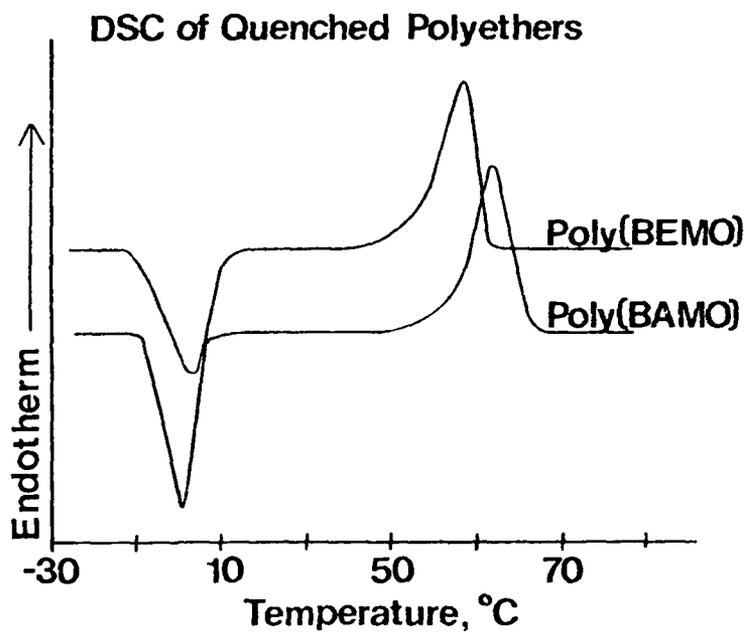
FIGURE 3

DSC of Poly(BEMO) Isothermally
Crystallized at Indicated Temperature
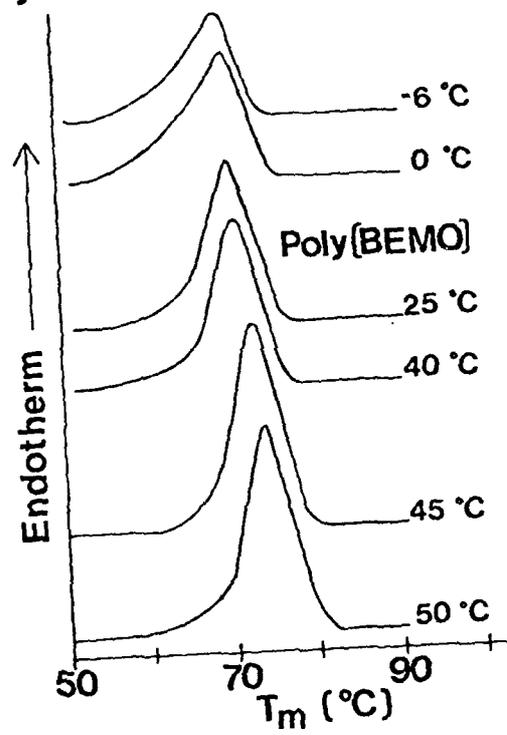
FIGURE 4

Poly(BEMO) Crystallized in
Solution at Indicated Temperature
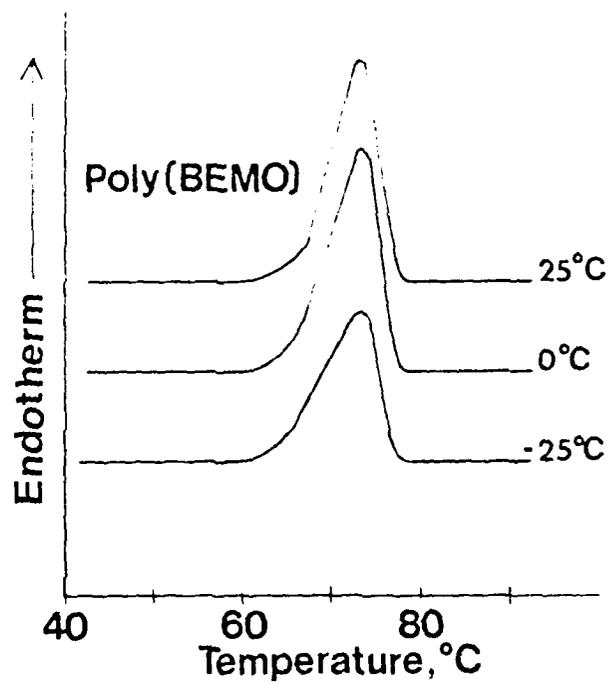
FIGURE 5

Enthalpy of Fusion
Determination by Diluents

Poly(BEMO)-DBP Mixtures
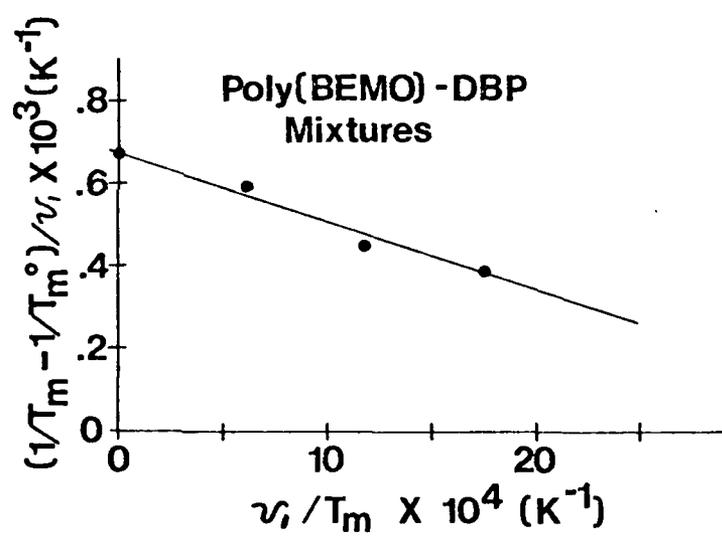
FIGURE 6

Equilibrium Melting Point
Plot of T_m vs. T_c
for Poly(BEMO)
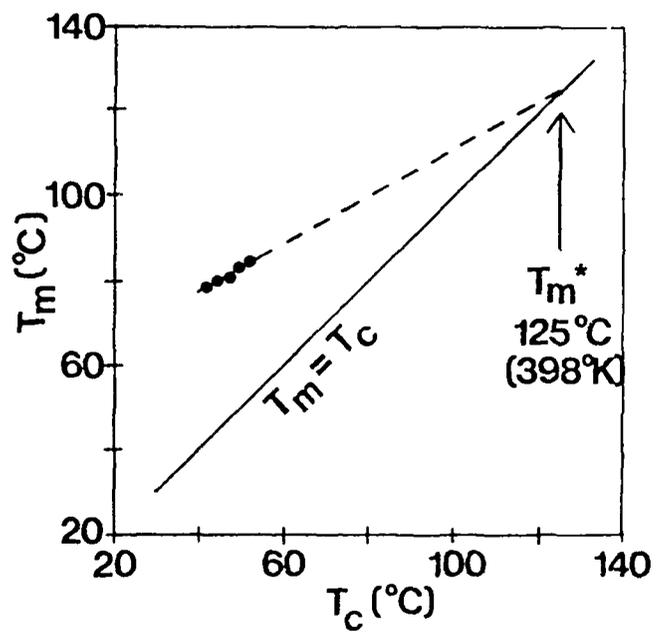
FIGURE 7

## Poly(BEMO) Crystal Modifications
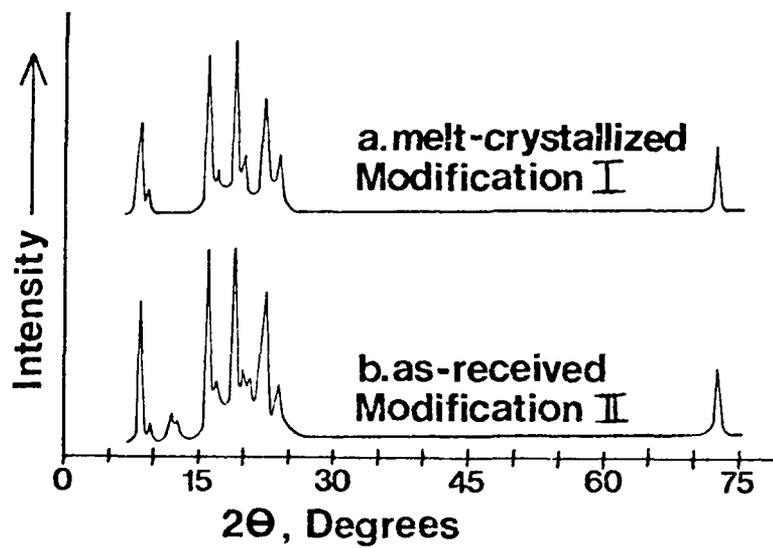
FIGURE 8

Poly(BAMO) X-Ray Scan
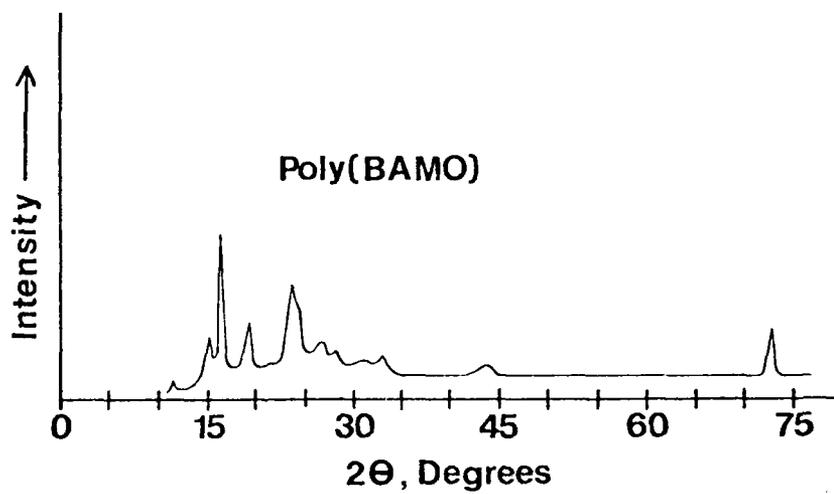
FIGURE 9

END

FILMED

1-85

DTIC